

International Journal of Remote Sensing

Publication details, including instructions for authors and subscription information:

<http://www.tandfonline.com/loi/tres20>

Monitoring and modelling land surface dynamics in Bermejo River Basin, Argentina: time series analysis of MODIS NDVI data

V. Barraza^a, F. Grings^a, M. Salvia^a, P. Perna^a, A.E. Carbajo^b & H. Karszenbaum^a

^a Instituto de astronomía y física del espacio (IAFE-CONICET-UBA), Grupo de Teledetección Cuantitativa, Buenos Aires, Argentina

^b Ecología de Enfermedades Transmitidas por Vectores, Prov. Buenos Aires, Argentina

To cite this article: V. Barraza, F. Grings, M. Salvia, P. Perna, A.E. Carbajo & H. Karszenbaum (2013): Monitoring and modelling land surface dynamics in Bermejo River Basin, Argentina: time series analysis of MODIS NDVI data, *International Journal of Remote Sensing*, 34:15, 5429-5451

To link to this article: <http://dx.doi.org/10.1080/01431161.2013.791759>

PLEASE SCROLL DOWN FOR ARTICLE

Full terms and conditions of use: <http://www.tandfonline.com/page/terms-and-conditions>

This article may be used for research, teaching, and private study purposes. Any substantial or systematic reproduction, redistribution, reselling, loan, sub-licensing, systematic supply, or distribution in any form to anyone is expressly forbidden.

The publisher does not give any warranty express or implied or make any representation that the contents will be complete or accurate or up to date. The accuracy of any instructions, formulae, and drug doses should be independently verified with primary sources. The publisher shall not be liable for any loss, actions, claims, proceedings, demand, or costs or damages whatsoever or howsoever caused arising directly or indirectly in connection with or arising out of the use of this material.

Monitoring and modelling land surface dynamics in Bermejo River Basin, Argentina: time series analysis of MODIS NDVI data

V. Barraza^{a*}, F. Grings^a, M. Salvia^a, P. Perna^a, A.E. Carbajo^b, and H. Karszenbaum^a

^a*Instituto de astronomía y física del espacio (IAFE-CONICET-UBA), Grupo de Teledetección Cuantitativa, Buenos Aires, Argentina;* ^b*Ecología de Enfermedades Transmitidas por Vectores, Prov. Buenos Aires, Argentina*

(Received 19 June 2012; accepted 21 March 2013)

The purpose of this work was to monitor and model land surface phenology over the past ten years in the South American Bermejo River basin using the Moderate Resolution Imaging Spectroradiometer (MODIS) normalized difference vegetation index (NDVI) product. In order to do this, we evaluated the characteristics of the satellite data and information available on the study area's ecosystem to choose the best model to capture the temporal dynamics of NDVI in local vegetation (sufficiently complex to provide a good fit and simple enough so that each parameter has an immediate ecological meaning). An ecological interpretation of model parameters was provided. Different land surfaces showed distinct fluctuations over time in NDVI values, and this information was used to improve object-oriented classification. A decision tree classification was developed to identify spatial patterns of NDVI functional form and the fluctuations that these patterns presented from 2000 to 2010. We integrated inter-annual information in a final map that distinguishes stable areas from changing sites. Assuming that large inter-annual spatial-scale fluctuations were related to climatic events, we established how vegetated land surfaces within the study area responded to these. Our study was designed to emphasize the interpretation of the spatial and temporal scales of land surface phenology.

1. Introduction

Time series of the normalized difference vegetation index (NDVI) have been used in several phenology studies to describe recurring patterns of vegetation dynamics by deriving multiple seasonal NDVI curve parameters. Examples of these parameters include the rate of increase and decrease of NDVI and the dates of the beginning, end, and peak of the growing season (Julien and Sobrino 2009; Pettorelli et al. 2005; Reed et al. 1994). One main assumption in this kind of analysis is that NDVI is a proxy for vegetation phenology. In this framework, land surface phenology (LSP) is defined as the seasonal pattern of vegetated land surfaces observed from remote-sensing platforms (Tan et al. 2011). LSP integrates phenological patterns (mainly spatial) and processes (mainly temporal) within heterogeneous biophysical environments across multiple scales (Liang and Schwartz 2009). Here, we are interested in using the NDVI time series to monitor LSP in order to detect temporal changes in vegetation condition. By definition, LSP can change mainly because of climatic variation (Myneni et al. 1997; Tucker et al. 2001; Zhou et al. 2003), non-climatic factors

*Corresponding author. Email: vbarraza@iafe.uba.ar

(e.g. fires, earthquakes (Giglio et al. 2003)) and/or as a result of anthropic disturbances (Clark et al. 2010).

Previous research used time series of vegetation indices to study land-cover change using multitemporal data (Pettoirelli et al. 2005). The Advanced Very High Resolution Radiometer (AVHRR) NDVI time series has been successfully used to monitor the inter-annual variability of global vegetation activity and to relate the vegetation's large-scale inter-annual variations to climate (Sobrino and Julien 2011; Myneni et al. 1997). The Moderate Resolution Imaging Spectroradiometer (MODIS) currently provides several vegetation index products that are widely used in environmental studies worldwide (Revadekar, Tiwari, and Kumar 2012). In general, optical remote-sensing measurements are influenced by atmosphere effects, clouds, and viewing geometry (Hird and McDermid 2009). This product is produced globally for every 16 day observation period at different spatial resolutions (Vermote and Vermeulen 1999). Due to the procedure used to generate this product, it features several characteristic artefacts which need to be identified and removed in order to provide a sound ecological interpretation. Removal of these artefacts is done using a quality layer, which provides relative quality information for each pixel in the 16 day composited NDVI data (Vermote and Vermeulen 1999).

The development of algorithms that are capable of automatically retrieving LSP metrics from NDVI time series data has been a popular research topic. Several models have been developed to estimate phenology metrics from NDVI time series, from simple linear smoothing methods (de Beurs and Henebry 2005) to more complicated analytical curve function methods (Alhamad, Stuth, and Vannucci 2007; Zhang et al. 2003). One of the most popular models to retrieve phenological parameters from satellite time series is TIMESAT (Jönsson and Eklundh 2004; Tan et al. 2011). The main approach of this model is to preprocess the observed time series in order to remove noise in satellite time series and to derive meaningful parameters of the temporal trend. In particular, it implements advanced smoothing functions to fit time series data, an outlier removal procedure, and provides a comprehensive set of phenology metrics as outputs. Another typical approach is the use of autoregressive models (AR, ARMA, ARIMA, etc.), which are linear prediction techniques that attempt to predict an output of a system based on previous system outputs. In the case of NDVI, current NDVI is modelled as a linear combination of past NDVI values (Box and Jenkins 1976; Fernández-Manso, Quintano, and Fernández-Manso 2011). Autoregressive models have the potential to extract seasonality information and to study the resilience of the vegetation. All these approaches show inherent virtues and weaknesses, but in the end, the quality of the data and the modelling objective are the factors that determine the success of a particular modelling approach.

In this article, we showed how MODIS NDVI data can be used to monitor LSP in the Bermejo River basin. For this purpose, a descriptive analysis of the study area's NDVI time series was made (autocorrelation and spectrum analysis) and several modelling strategies were tested. Our methodology has three associated objectives: (1) to understand model parameters in terms of LSP; (2) to map the annual dynamics of the data, defining NDVI functional forms related to annual performance of the land surface in the study area; and (3) to map the inter-annual dynamics of the NDVI functional forms as a way to monitor environmental changes.

2. Study area

The Bermejo River basin (see Figure 1) has its head in the Andes Mountains of north-western Argentina and southern Bolivia. The basin extends over about 123,000 km². This region was mentioned as a hot spot of land cover change by Baldi et al. (2008). The variable

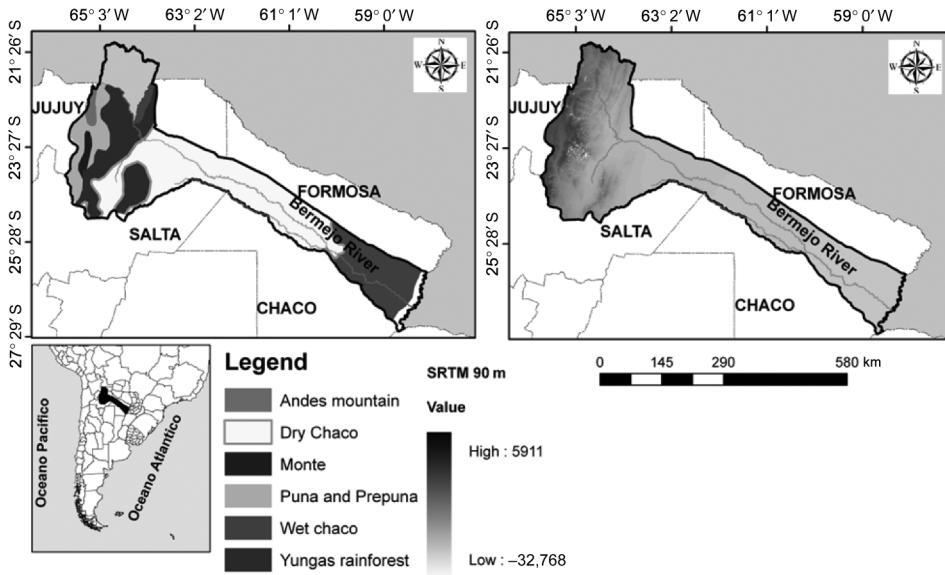


Figure 1. Ecoregion and SRTM image of the Bermejo River basin.

weather and topographic conditions in this large basin promote an array of rain forests, humid valleys, and mountain deserts in the upper basin, and both dry and humid and gallery forests in the lower basin. The basin covers two phytogeographic forested areas whose conditions may affect land surface NDVI patterns.

- The Great Chaco is a unique dry subtropical forest, occupying the middle-lower area in the Bermejo River basin. It can be subdivided into two regions, known as the Dry Chaco and Humid Chaco (Minetti 1999). The Dry Chaco presents a mean annual rainfall of ~ 700 mm, which differs from the ~ 1300 mm of the Humid Chaco. Precipitation and hydrological anomalies affect the Humid more than the Dry Chaco, the vegetation of the latter being adapted to rainfall stress and temperature variation. The vegetation in the Dry Chaco consists of mixed xenophile forests dominated by deciduous or semi-deciduous species, and shows a stationary growth season related to the rainfall pattern (Morello 1968). The Humid Chaco is characterized by mixed xenophile forests and the presence of aquatic habitats (estuaries, etc.), whose phenology is influenced by climatic conditions and flood pulses. Both areas are classified as open dry forest (20% of tree crown cover) with two strata (UMSEF 2006).
- The Tucuman-Bolivian forest or Yungas ecoregion is located in the upper basin. The wet and humid climate is influenced by the northern trade winds, and annual rainfall typically exceeds 2500 mm (Cabrera 1976). It is characterized by a strong altitudinal gradient, which corresponds to an important gradient in vegetation species. Along this gradient, the vegetation has different adaptations to environmental conditions (drought, higher temperatures, and frost and snow in winter). This region presents more layers (three strata) and coverage percentage (30% tree cover) than the Chaco Plain.

The basin climate is subtropical, with a mean annual rainfall cycle showing a minimum in winter, which is more pronounced in the west, with dry conditions prevailing from May to September (González and Barros 1998; Reboita et al. 2010). Subtropical South America

is known as a region with an important El Niño–Southern Oscillation (ENSO) signal in the precipitation field (Kiladis and Diaz 1989; Ropelewski and Halpert 1987). This signal varies along each of the ENSO phases, and differs among regions (Grimm, Barros, and Doyle 2000). In this region, the annual cycle of flooding starts in the framework of a cool phase, called La Niña, ENSO.

3. Data and methods

3.1. Data set and pre-processing

Taking into account that NDVI performs better than the enhanced vegetation index (EVI) in regions of sparse vegetation (Huete et al. 2002), we decided to use the NDVI from MODIS product at 250 m spatial resolution (MOD13Q1). We evaluated this decision using basic statistics and our general expertise in the area. MODIS NDVI 16 day composite grid data are available in HDF format, in sinusoidal projection over spatial units called tiles of $10^\circ \times 10^\circ$ (<https://wist.echo.nasa.gov/api/>). The timeframe of the analysis was between February 2000 and December 2010, the scene used was h12v11 to cover the entire study area and the total number of images analysed was 250. Using quality assurance (QA) information, we filtered low-quality data (less than intermediate, $QA < 7$). The images were re-projected from sinusoidal to geographic projection (datum WGS 84). Surface reflectance products, such as MYD13/MOD13 data (Vermote et al. 1997; Vermote, El Saleous, and Justice 2002), are generated globally but are divided into tiles in the sinusoidal (SIN) projection (Wolfe, Roy, and Vermote 1998). Being a global projection, the SIN projection introduces substantial distortion in areas away from the central meridian, which in the case of MODIS is the Greenwich Meridian or 0° longitude. This is especially noticeable over the mid-latitude. Furthermore, the study area covers a region much larger than a single Universal Transversal Mercator (UTM) zone and national projection (Argentine Gauss Krüger System = 4 zones), so geographic projection was selected.

The MODIS vegetation index composition algorithm operates on a per-pixel basis and relies on multiple observations over a 16 day period to generate the product (Huete, Justice, and Leeuwen 1999; Vermote and Vermeulen 1999). The MOD13Q1 compositing algorithm uses three aggregation strategies: bidirectional reflectance distribution function composite (BRDF-C), constrained view angle-maximum value composite (CV-MVC), and maximum value composite (MVC). The technique employed depends on the number and quality of the observations (Huete et al. 2002; Vermote and Vermeulen 1999).

Besides remote-sensing data sets, we also used meteorological data from the Bermejo River basin. Precipitation data were continuously monitored for the period 2000–2010 at five, nine, and seven stations along the upper, middle, and lower basin, respectively. Furthermore, we used a deforestation land-cover map from UMSEF (2006) based on visual interpretation of Landsat 5 TM and 7 ETM images. The land-cover classes used in this work are Forest Land (land with tree crown cover $>20\%$), Other Wooded Land (land with tree crown cover of 5–20%), and Other Land (which includes agricultural land, meadows and pastures, built-up areas, and barren land, among others). Land-cover classes are based on crown cover and physiognomic features, according to Forest Resources Assessment (FAO) classification and adapted to Argentinean characteristics. This map was validated with ground truth (UMSEF 2006).

3.2. Time series characteristics

In our study area, NDVI time series presented strong seasonal patterns (see Figure 2). Temporal NDVI dynamics follows broad phenological phases such as onset greenness,

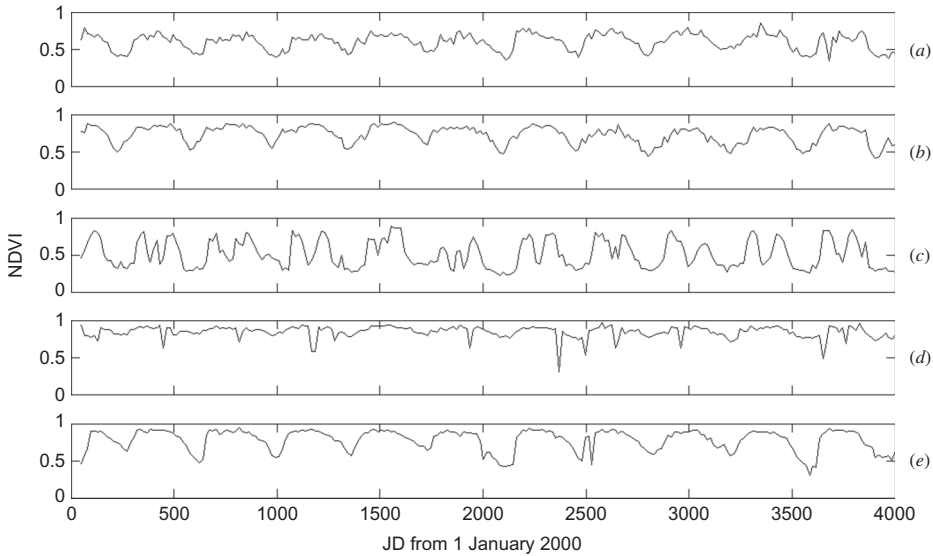


Figure 2. Examples of NDVI time series of the study area. (a), (b), (d), and (e) natural vegetation; (c) crop area.

peak greenness, and senesce period. In natural vegetated areas (see Figures 2(a), (b), (d), and (e)), NDVI exhibits a parabolic trend, with a maximum in summer and minimum in winter. Non-natural vegetation shows annual or biannual profiles that are related to crops and grazing areas (see Figure 2(c)).

Abrupt changes in NDVI values were reported in different studies and can be related to extreme events (e.g. burning, flooding), but in our study area, these were usually related to atmospheric contamination. After removal of atmospherically noisy data using the QA ancillary information, NDVI trends still showed non-negligible intersample (16 day) variability (see Figure 2). This variability cannot be related to ecosystem changes, since these extreme, rapid changes in phenology were not observed. Since they are more likely related to NDVI compositing methodology, we evaluated the techniques used to generate the NDVI data in the study area at both spatial and temporal scales, with the aim of understanding which portion of the NDVI temporal behaviour could be related to the compositing methodology. To this end, using the information in the quality assessment (QA) layer, we extracted the information about the compositing methodology for each pixel and date.

We found that in spite of being labelled 'check quality', in general, most NDVI values were generated using the BRDF compositing methodology. In the upper basin, the BRDF model was used in 80–100% of the pixels, and in the middle-lower basin about 90–100%. In the upper basin (cloudy forest region), the compositing methodology usually changed to CV-MVC during the rainy season (December to May). This is expected, since cloud-contaminated pixels increase to a point where for a given pixel, there are fewer than five clear days in the 16 day period. When this happens, observed NDVI values present a systematic bias of ~ 0.2 (Moody et al. 2005; Xiao et al. 2003). However, in the majority of the study area, NDVI high-frequency noise is not dependent on changes in aggregation methodology.

Nevertheless, several artefacts in the BRDF aggregation technique, mostly related to the BRDF algorithm hypothesis, have been reported. For example, when simulating NDVI

as seen by MODIS at 250 m using the Walthat BDRF model, Leeuwen et al. (1997) found a discrepancy between simulated and observed NDVI values of ~ 0.011 and ~ 0.008 for Fallow and Aspen forest, respectively. This discrepancy is related to the fact that actual forest BDRF is more complex than that in the Walthat model. In our study, the mean value of NDVI uncertainties was ~ 0.01 , which agrees with the results of Leeuwen et al. Moreover, the Walthat model is known to incur problems in modelling the BDRF of open complex canopies (Walthall 1997), like those of the Chaco Forest. Therefore, we propose that the observed high-frequency noise in the NDVI of our study area is an artefact related to BDRF aggregation methodology. BDRF failed to estimate nadir NDVI using off-nadir acquisitions, since BDRF in this area was significantly different from that proposed by Walthat.

In order to better characterize the time series properties, a simple frequency spectrum was analysed (results not shown); this spectrum shows a strong annual component and higher frequency components in certain noisy areas. In general, no inter-annual trends were observed. To examine repeating patterns along the time series, we evaluated the autocorrelation function of the data; this function shows time dependency, which can indicate a non-stationary process (i.e. the future values of NDVI are strongly influenced by those of both the present and the past). These results suggest that NDVI time series for this area are highly complex, since they exhibit seasonal patterns with significant noise. The annual behaviour is mostly due to phenology, and the high-frequency events can be related to (1) sporadic short-term vegetation hydrologic stress and (2) noise due to the composite algorithm. Therefore, it is mandatory to evaluate the causes of these high-frequency events before trying to estimate LSP metrics from these data.

3.3. NDVI time series model

Taking into account the previous analysis (Section 3.2), the most promising approach is to model NDVI annual variation in terms of LSP variation without over-fitting noise in the data. In this context, we evaluated simpler polynomial models, since they are intrinsically capable of modelling NDVI annual trends. A second-order polynomial model was selected, since this has the advantage of being sufficiently complex to provide a good fit ($R^2_{\text{adj}} = 72.86\%$) and is sufficiently simple that each parameter has an immediate ecological meaning (see Table 1). Several authors (e.g. de Beurs and Henebry 2005) successfully used polynomial algorithms to model vegetation dynamics in boreal forest, and the model used in this work is a modification of the algorithm proposed by these authors:

$$\text{NDVI}_{\text{fit}} = \alpha + \beta \text{NDVI}(t) + \gamma \text{NDVI}(t)^2,$$

Table 1. Description and ecological interpretation of model parameters.

Model parameter	Ecological interpretation	Comments
α [NDVI]	Proportional to the amount of green biomass at the beginning of the observation period (winter)	Always a positive value between zero and one
β [NDVI/ t]	Initial growth rate of green biomass	Always a positive value
γ [NDVI/ t^2]	Determines the shape of the curve, with smaller values producing broader curves. Related to the concavity of the annual trend	Always a negative value

Notes: Units of model parameters are mentioned between brackets. t is the Julian day.

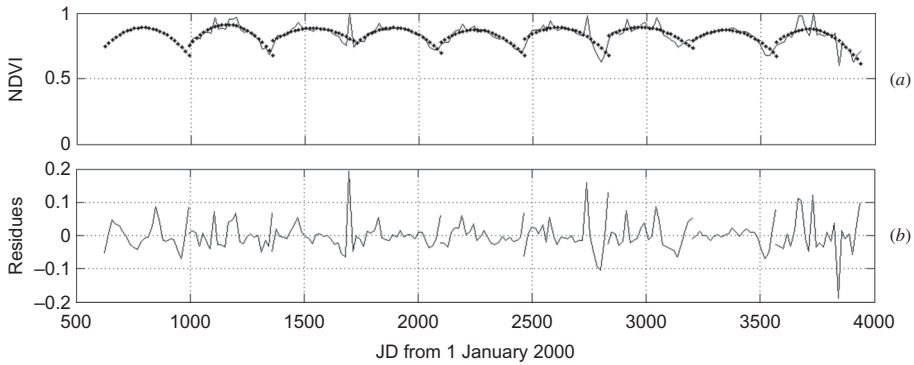


Figure 3. Example of 16-day MODIS NDVI time series containing (lines) estimated seasonal values ($NDVI_{fit}$, line) (a) and residues series (b).

where α is the intercept of the NDVI pattern, β is its initial slope, γ is its concavity, and t is the Julian day (see Table 1). The starting period for each year is taken as the start of winter, so it coincides with the vegetation cycle. NDVI data were fitted for each growing season (see Figure 3).

Well-fitted regression models should result in residuals normally distributed with zero mean. In general, the proposed model fits the NDVI data of the study area, considering that the average residues are small. In this context, the parameters used to define these classes were adequate to capture NDVI annual trends. Finally, it was considered that areas with residue >0.1 were characterized by an annual pattern that could not be explained by a quadratic model, and were labelled 'non-parabolic trends'. This threshold was arbitrarily chosen in order to eliminate trends presenting simple seasonal dynamics from the analysis.

3.4. Decision tree classification

The NDVI LSP model selected characterizes a given year using a set of model parameters. However, unrealistic combinations of parameters were filtered, since they correspond to clusters of pixels with similar LSP model parameters that are not ecologically possible (see Table 1). For example, a negative initial slope (beta parameter) and a positive gamma parameter result in a convex curve. In order to identify the phenological patterns in the Bermejo River basin, we analysed 400 random points from different land covers presenting a minimum inter-point distance of 20 km. From the analysis, main NDVI 'seasonal patterns' were identified and a set of 'seasonal pattern classes' was defined as a function of model parameters. Figure 4 shows examples of the four most common NDVI profiles found in the area. NDVI patterns in which it was not possible to identify a parabolic annual trend were related to either (1) highly disturbed vegetation, (2) water, (3) bare soil, or (4) crops (abnormal annual or biannual behaviour).

For natural vegetation, it was possible to make an ecological interpretation of each class in terms of NDVI functional forms. This interpretation was itself based on the mean values of model parameters (see Table 1). Using this information, four classes of NDVI functional forms were defined.

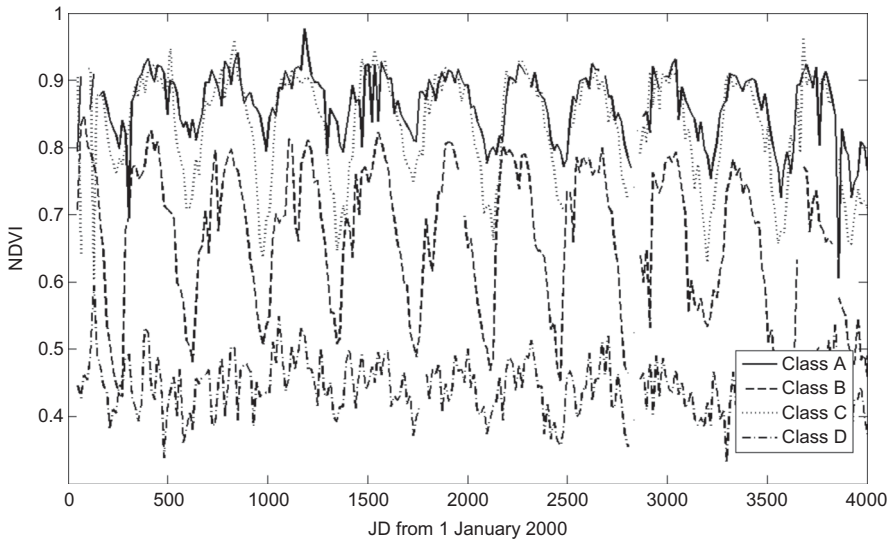


Figure 4. Main NDVI patterns found in the area (see Section 3.4 for class description).

- Class A: High photosynthetic biomass at the beginning of the growing period, low seasonal variation (low slope at the beginning of the growing season and low concavity).
- Class B: Low photosynthetic biomass at the beginning of the growing period, high seasonal variation (high slope at the beginning of the growing season and low concavity).
- Class C: High photosynthetic biomass at the beginning of the growing period, high seasonal variation (high slope and low concavity).
- Class D: Low photosynthetic biomass at the beginning of the growing period, low seasonal variation (low slope at the beginning of the growing season and high concavity).
- No class: parabolic annual curve that did not present a straightforward ecological interpretation.
- Water: Non-parabolic curve with a random annual performance.
- Residues >0.1 : Non-parabolic curve.

Classes A and C showed higher NDVI values throughout the year, but Class A had weak seasonal variation compared with Class C. Class B had the highest slope and the shortest growing season. Finally, Class D showed an annual trend similar to Class A, but with lower NDVI values. These descriptions roughly correspond to deciduous (Classes B and C) and semi-deciduous (Classes A and D) areas. Additionally, Classes C and A showed higher green biomass during the year than the other classes. Class definitions are graphically sketched in Figure 5.

The classification scheme presented above helped to characterize the intra- and inter-class variability of phenological patterns in the study area. Distance-based per-mutational multivariable analysis of variance (PERMANOVA, Anderson 2001) was used to analyse the multivariate assemblage data for the complete multi-factor design. Data from all sample

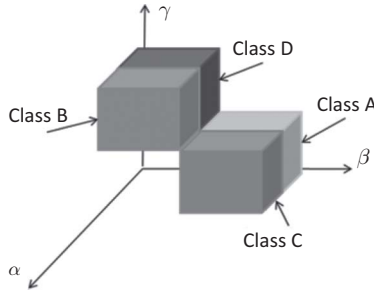


Figure 5. NDVI functional form classification definition in the alpha, beta, gamma space.

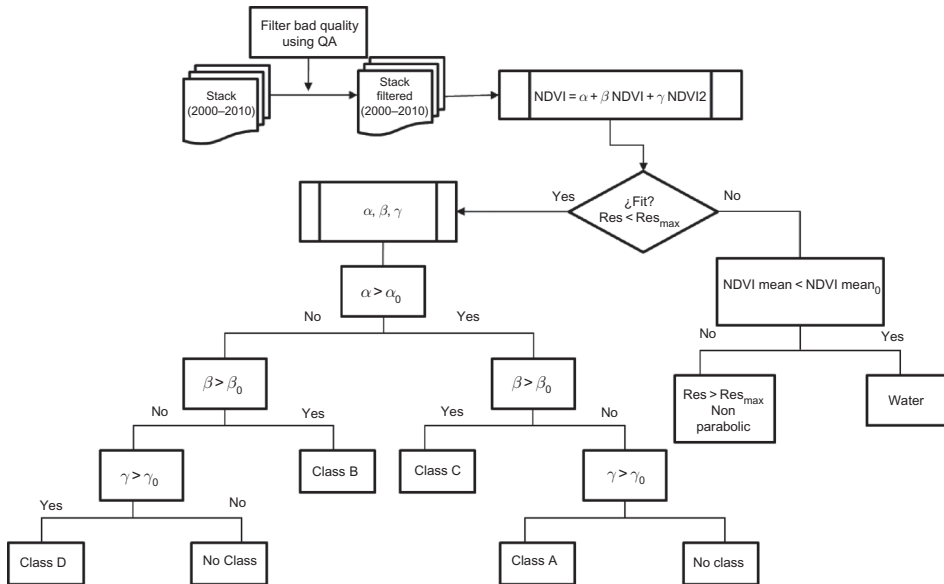


Figure 6. Schematic diagram of the decision tree classification used. $\beta_0 = 0.002$, $\gamma_0 = -0.7 * 10^{-5}$, $\alpha_0 = 0.6$, $R_{max} = 0.1$ and $NDVI\ mean_0 = 0.30$.

periods were analysed together, with class type as fixed factors. *P*-values for the test statistic (pseudo *F*-value) were based on 10,000 permutations of raw data.

Since model parameters have a straightforward ecological interpretation, a supervised classification is the natural choice in order to preserve a clear ecological interpretation of the resulting classification. A decision tree classification was chosen due to its substantial advantages in supervised classification problems (Friedl and Brodley 1997); in particular, they are strictly nonparametric and do not require assumptions regarding the distributions of the input data, which are difficult to meet in complex environments. The classification algorithm flowchart is sketched in Figure 6.

3.5. Time series change detection

An analysis of the recent progress in time series analysis of biophysical variables reflects the necessity to develop standard models to capture series dynamics and evolution (Verbesselt

et al. 2010). In particular, the detection of structural changes is particularly important. A structural change in a time series occurs when there are temporary or permanent changes in one or more components of the model or model parameter (Verbesselt et al. 2010). Since NDVI is a proxy for vegetation phenology, a structural change in NDVI time series has relevant ecological implications. Changes in vegetation phenology affect the carbon and water cycles and energy fluxes through photosynthesis and evapotranspiration.

To this end, a time series change detection methodology was designed to look for changes in the NDVI functional forms. In our terminology, a change occurs when LSP changes from one NDVI functional form to another. Using this definition, the following relevant questions were addressed.

- (1) What type of variations is detectable in MODIS NDVI series?
- (2) How many changes took place from 2000 to 2010? What was the temporal profile of these changes?
- (3) Are these changes related to environmental and/or anthropic drivers?

In order to answer these questions, two metrics were adopted. First, the number of transitions between classes was evaluated (class number index (CNI)). This value should be related to pixel temporal stability, and will be useful to identify the temporal dynamics of every pixel in the period analysed. Second, the number of distinct classes on which each pixel was classified from 2000 to 2010 was computed (class change index (CCI)). This second metric is complementary to the previous, and is useful to characterize the specific dynamics of every pixel. Finally, using these two metrics, the changes in the seasonal behaviour of LSP were evaluated. The two main sources of variations capable of producing changes in NDVI functional forms are environmental (precipitation, temperature, evapotranspiration, etc.) and anthropic (deforestation, selective logging, livestock grazing, etc.). We hypothesize that the large spatial changes in NDVI functional forms are mostly related to large environmental variations. On the other hand, NDVI temporal trends of smaller spatial extent will be related to anthropic forcing (mainly deforestation).

Figure 7 shows the complete scheme of our analysis methodology. The analysis is divided into four sections. The first corresponds to characterization of time series properties, identifying sources of noise and the annual tendency of the data (Section 3.2). The second corresponds to the extraction of model parameters from the NDVI annual trend (Section 3.3). The third describes the classification of model parameters into NDVI temporal trend classes (Sections 3.4 and 4.1). The final section describes the analysis of NDVI temporal trend dynamics using auxiliary data (precipitation), in order to associate it with climatic forcing (Section 4.2), and the correspondence between NDVI non-parabolic trend and deforestation land-cover types (UMSEF 2006).

4. Results

4.1. Classification results

Figure 8 shows the annual classification results. In every year of the study period, more than 90% of the study area presented a parabolic trend which was associated with natural vegetation. Moreover, four NDVI functional forms (Classes A, B, C, and D) could explain most of the vegetation LSP seasonal patterns present in the Bermejo River basin. The remaining ~10% corresponded to the non-parabolic annual behaviour of NDVI. Comparing classification results, differences are evident between the upper, middle, and lower regions of the

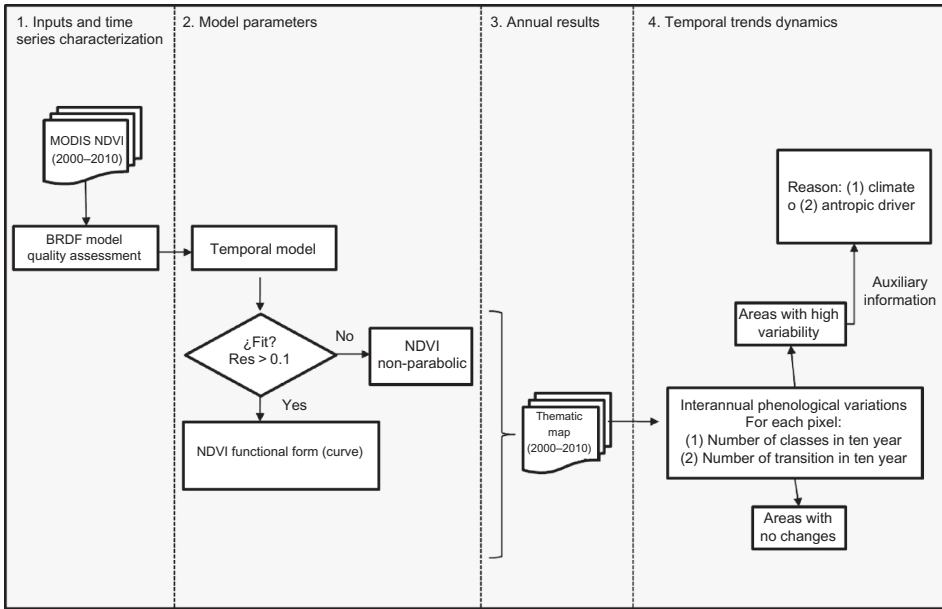


Figure 7. Flowchart of the complete methodology.

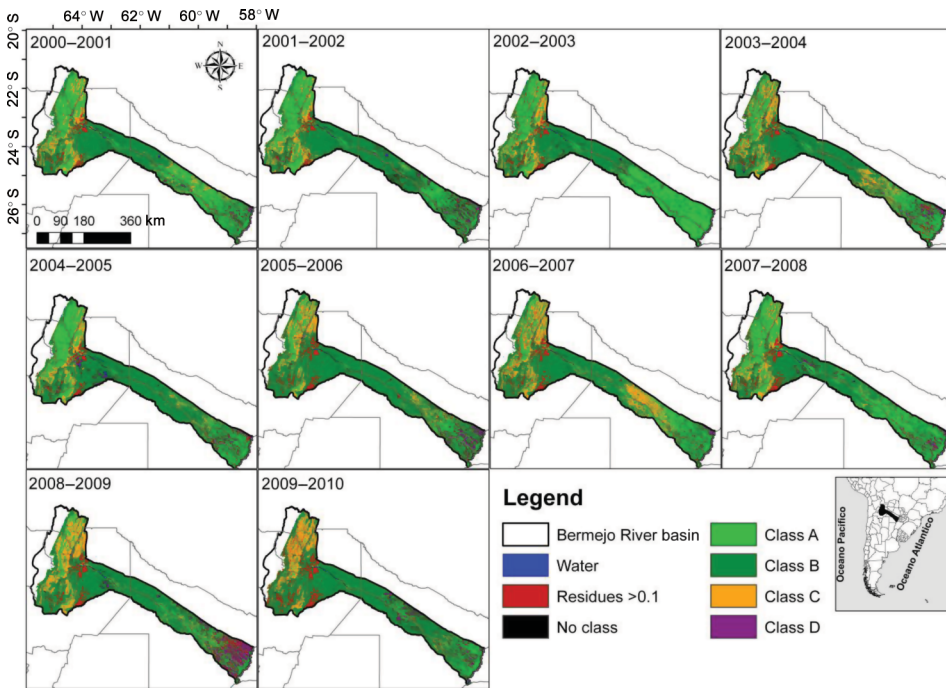


Figure 8. Annual classification results, 2000-2010.

basin. NDVI functional forms with strong seasonality (B and C) were present mainly in the middle basin, while classes with weak seasonality (A and D) were found in the lower and upper basin.

The results of PERMANOVA show significant differences among the four groups of NDVI functional forms ($p < 0.05$, $df = 3$). Class B showed the largest intra-class variability in terms of model parameters, but it was not possible to establish statistically significant subgroups.

Interclass variability during the study period was low, because $\sim 60\%$ of the middle basin area was systematically categorized as Class B. This is evidence of the stability of the middle basin in terms of NDVI functional form during the study period. Inter-annual fluctuations occurred mainly in the upper and lower basin. Differences between Class A and D were observed in the lower basin, and between A and C in the upper basin. To carry out a deeper analysis of these transitions, in the next section, we quantify the information obtained and compare it with the available precipitation and deforestation data.

4.2. Change detection analysis

Inter-annual dynamics were identified by analysing class changes from 2000 to 2010. As seen in Figure 8, the spatial structure of the observed changes was consistent with large patches of vegetation with similar annual dynamics.

In order to analyse these results, two indicators were defined. Figure 9 shows the number of different classes represented by each pixel over the study period (CNI). Since the

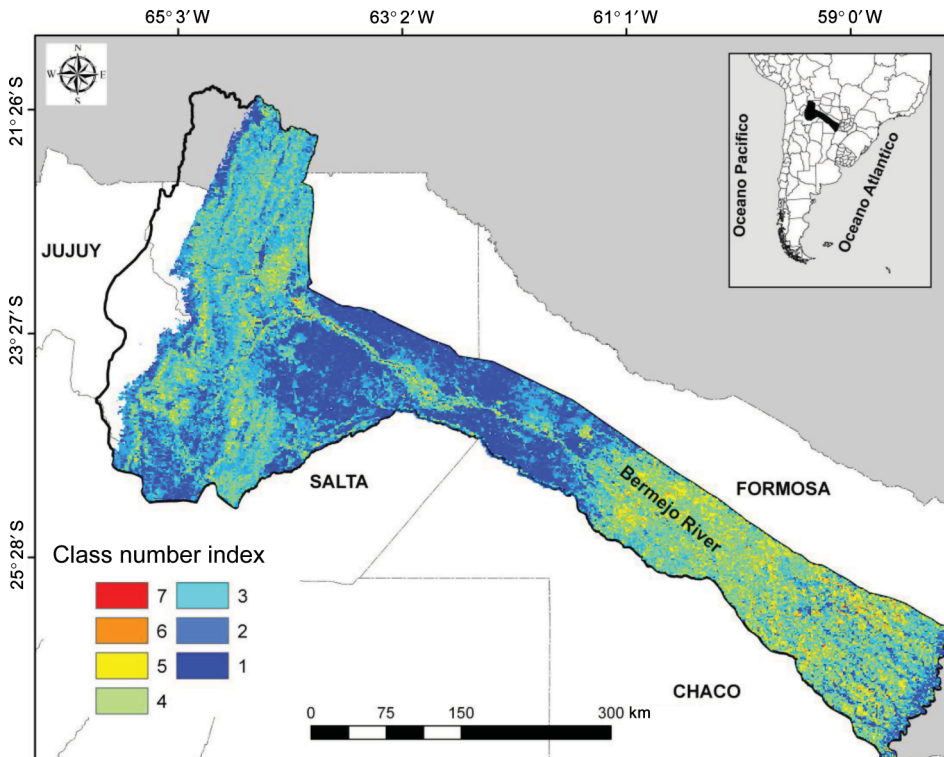


Figure 9. Class number index (CNI) for the study area.

number of different classes defined is seven (see Figure 8), this index varies in the range $1 \leq \text{CNI} \leq 7$. A pixel with a large CNI value is unstable between years in terms of NDVI functional forms; conversely, a pixel with low CNI (i.e. 1) presents no inter-annual change in the study period. In the CNI image, the three main subdivisions of the basin (upper, middle, and lower) are easily identified, which adds evidence to this particular regional segmentation. In the middle basin, the area presents large patches (to both sides of the Bermejo River) with CNI values of 1–2 for the 10 year study period. The upper basin was dominated by areas with CNI ~ 2 –4, while the lower basin had a mean CNI of ~ 4 .

The other indicator defined is the number of transitions presented by each pixel over the study period (CCI, see Figure 10). Since there are nine transitions from 2000 to 2010, this index varies between $1 \leq \text{CCI} \leq 9$. A pixel with a large CCI is unstable between years in terms of NDVI functional forms (but it can present a particular kind of instability); conversely, a pixel with low CCI (i.e. 1) presents no transitions in the study period. The CCI image shows that more than 60% of the middle basin has a CCI value of 0 or 1, which indicates a very stable area in terms of NDVI functional forms. In particular, in this section of the basin, the more dynamic sites were located in areas close to the river. The upper basin had CCI ~ 3 –4, related to CNI ~ 2 –3. The lower basin showed CCI ~ 4 –6, associated with CNI 3–5. As expected, the total number of transitions between classes (CCI) complements the data on class number variability (CNI).

Figure 11 illustrates the frequency of pixels for different combinations of CCI and CNI. By definition of these indices, there are combinations that cannot exist (above the dashed

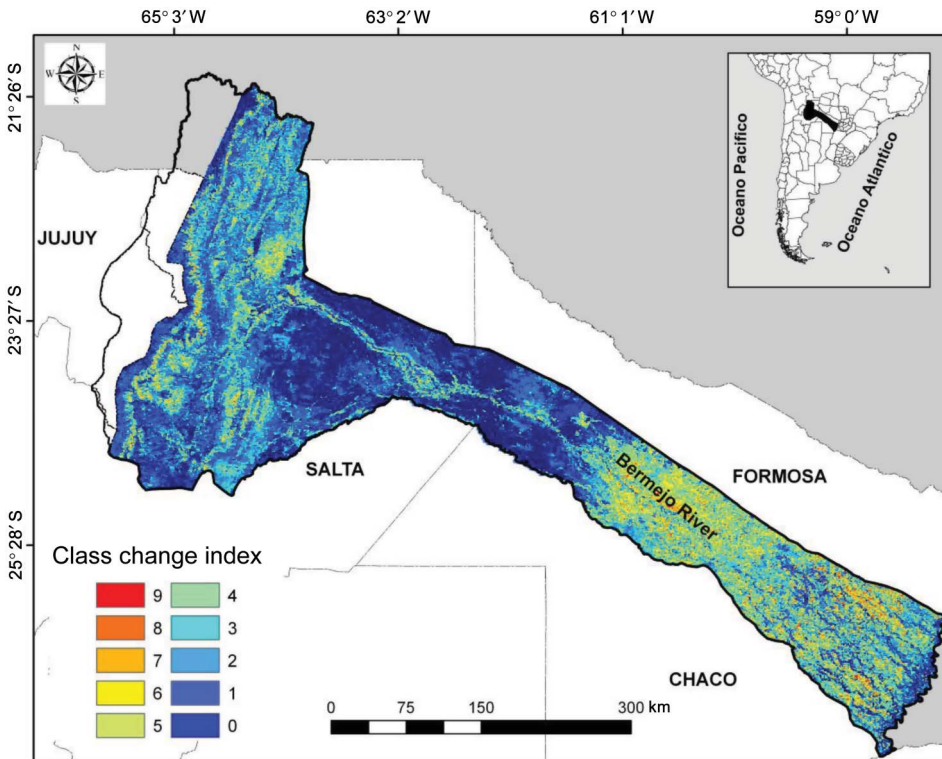


Figure 10. Class change index (CCI) for the study area.

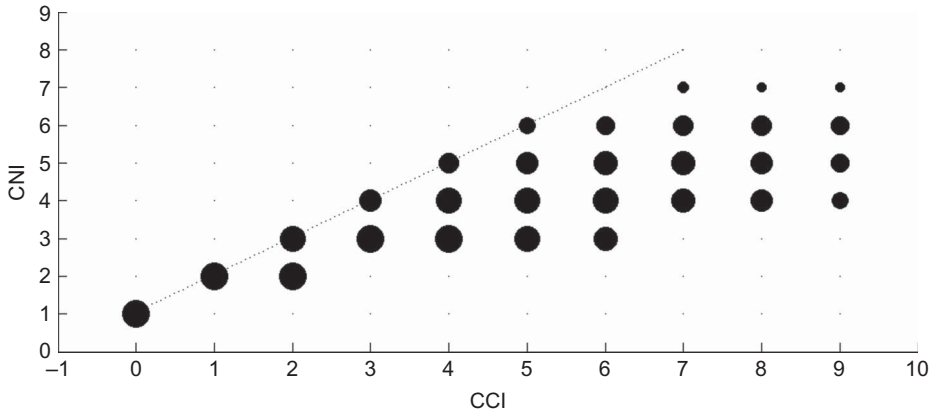


Figure 11. Scatter-plot between CNI and CCI. The size of the bubble is proportional to frequency in the logarithmic scale.

line). In the frame of LSP, CCI and CNI equal to 0 and 1, respectively, correspond to very stable areas with no response in terms of NDVI to climate forcing (similar NDVI profile through time). An area may be called resilient to environmental drivers when it has CCI and CNI = 1 and 2, respectively. Combinations between the ranges 6–9 for CCI and 2–3 for CNI were not observed. Based on these results, in the next section we will discuss the dynamics of the basin in relation to ecosystem and climate characteristics.

4.2.1. Areas where no changes in NDVI pattern were observed

An analysis was conducted to better understand, identify, and characterize stable areas showing no change in NDVI pattern (see Figures 12 and 13). The vegetation in the middle basin was mainly labelled as class B (low photosynthetic biomass at the beginning of the growing period and high seasonal variation), and either remained stable within this class or changed sometime over the study period and then returned to the same class (CNI = 1–2 or

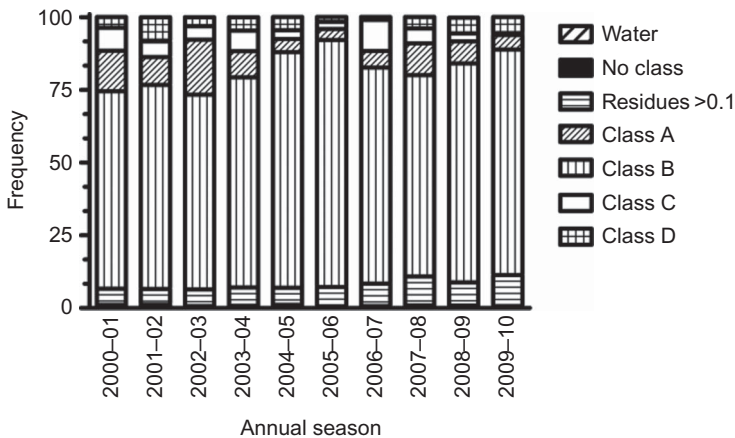


Figure 12. Class frequency for the study period.

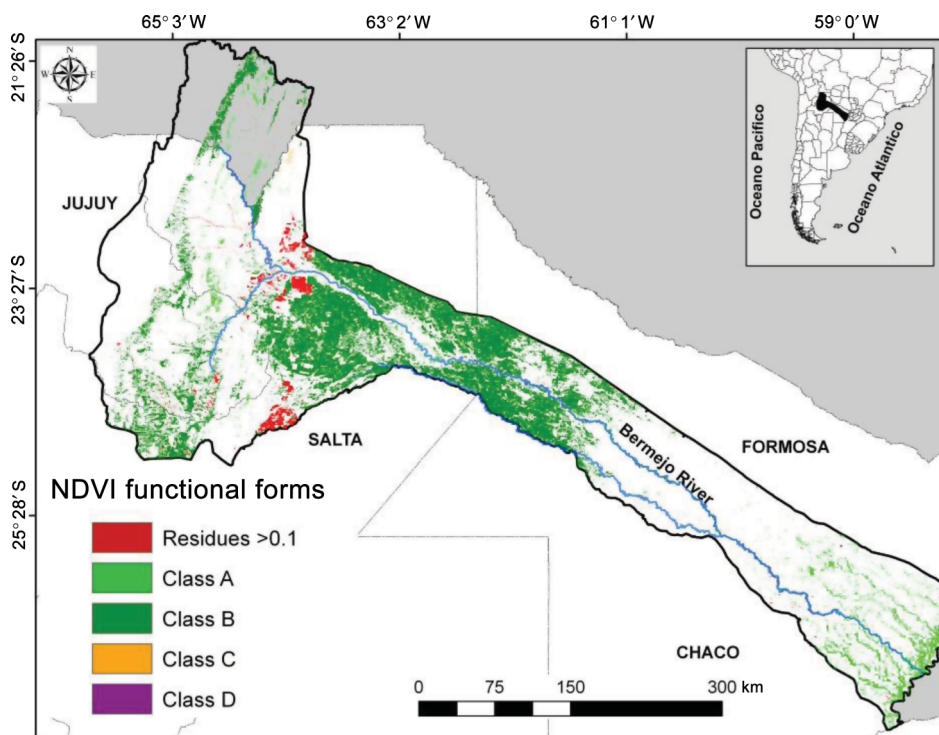


Figure 13. Stable areas for each class with the same NDVI functional form during the 10 year period 2000–2010.

CCI = 0–2). This is indicative of the system's strong resilience to environmental drivers (i.e. the capacity of a system to respond to a perturbation or disturbance – in this case, precipitation events – by resisting damage and recovering rapidly). This area belongs to the Dry Chaco ecoregion, in which the dominant vegetation (woody) is adapted to both significant fluctuations in water availability and temperature variations (xerophyte forest) (Morello and Adamoli 1974). This explains the high level of ecosystem resilience during the study period in regard to NDVI temporal profile. On the other hand, riverside sites in the middle basin did not remain stable ($CNI \leq 4$, $CCI \leq 5$). The vegetation pattern for this region is mainly dominated by the riverine forest, whose life cycle depends largely on hydrological and precipitation conditions (Torrella and Adámoli 2005), which in turn presents important inter-annual dynamics.

In the lower basin, which corresponds to the Humid Chaco ecoregion, only a small proportion of the area showed no change in NDVI pattern ($CNI = 1$). This area is located in the riverine forest ridges on the Paraguay–Parana River axis, characterized by the presence of permanent wetlands that depend on the Bermejo and Paraguay River dynamics. Physiognomically, the vegetation in this area consists of grasses, cyperaceous, and water hyacinth intermingling with the Forests of Ribera (Alberto 2005; Ginzburg and Adámoli 2005; Ginzbur et al. 2005). The high level of inter-annual fluctuation indicates a lower resilience of the system to climatic disturbances, which is related to the presence of a greater richness of aquatic habitats (estuaries, etc.) whose phenology is influenced by climatic conditions and flood pulse.

Something similar occurred in the upper basin, where the vegetation is characterized by a strong altitudinal gradient which correlates with a vegetation gradient (Brown et al. 2002). Depending on the altitudinal gradient level, some species are adapted to the most diverse environmental conditions (drought, high temperatures, high humidity, winter frost, and snow). This creates environmental conditions for the coexistence of species of different biogeographical origins along the altitudinal gradient. For this reason, this area includes both stable and variable areas.

The area located within the boundary between the upper and middle basins is characterized by intensive agricultural activity, and was mostly labelled as ‘no fit’ (residues >0.1). Selecting random samples along this area, we noticed a biannual cycle that represented crop areas (see Section 4.2.2). As a result, in the final section, we analyse the increase in this class area as a function of agricultural expansion.

In summary, stable areas (in terms of NDVI functional forms) are present along the whole Bermejo River basin. However, the middle basin presents the largest and most homogenous patches (Class B), which were resistant to the environmental forcing present during the study period (flood, drought, rain). This interpretation is grounded in the vegetation characteristics of the area (xerophyte forest) and in previous studies. Moreover, agricultural areas were also stable once established (red in Figure 13). Finally, some riverine forest in the lower basin showed a stable pattern.

4.2.2. Areas where changes in NDVI pattern were observed

As stated above, changes in inter-annual NDVI patterns should be related to environmental and/or anthropic forcing. Human-instigated fires have also played a role in the reduction of forest land cover, but in the lowlands, its importance has been secondary compared with that of agricultural expansion (Zak et al. 2008). Among the climate drivers, precipitation is the most important in this area (Barros, Castañeda, and Doyle 2000; Barros, González, et al. 2000; Cabido et al. 1993; Castañeda and Barros 1994; González, Castañeda, and Texeira Neri 2005). Thus, we analysed precipitation anomalies for several stations along the basin. Figure 14 summarizes annual precipitation anomalies for the three regions of the basin from September to August (i.e. closely associated with the growing season). Three major events can be identified:

- a reduction in mean annual precipitation during the period 2004–2005 in the middle and upper basins;
- a positive anomaly in annual precipitation during the period 2006–2007 over the whole basin; and
- a reduction in mean annual precipitation during the period 2008–2009 in the middle and lower basins.

From the analysis of annual classification results, it was possible to identify two large areas with moderate values of both CCI (~ 2 – 6) and CNI (~ 2 – 4). We identified these sites as the only important classes in terms of spatial extent (CNI ~ 2). In the lower basin, these two classes were A and D (see Figure 15). From 2001–2002 to 2002–2003, Class A increased to up to $\sim 80\%$ of the total area. Moreover, from 2007–2008 to 2008–2009, the frequency of Class A decreased with a concomitant increase in area of Class D. The mean difference between these two classes is the parameter α (biomass at the beginning of the growing season). A significant correlation coefficient was found between the mean value of

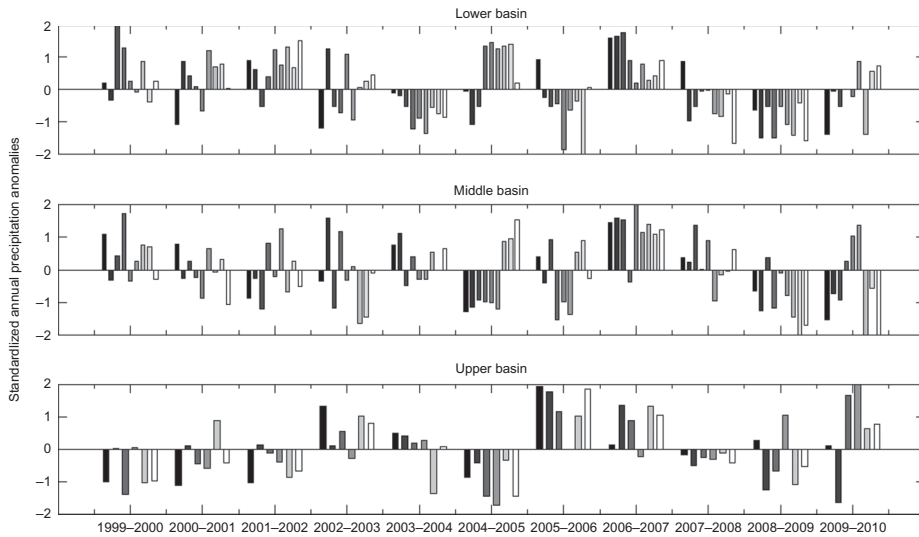


Figure 14. Standardized anomalies of annual precipitation (mm), 1999–2010, in the lower, middle, and upper Bermejo River basin. Differently shaded bars indicate different precipitation stations.

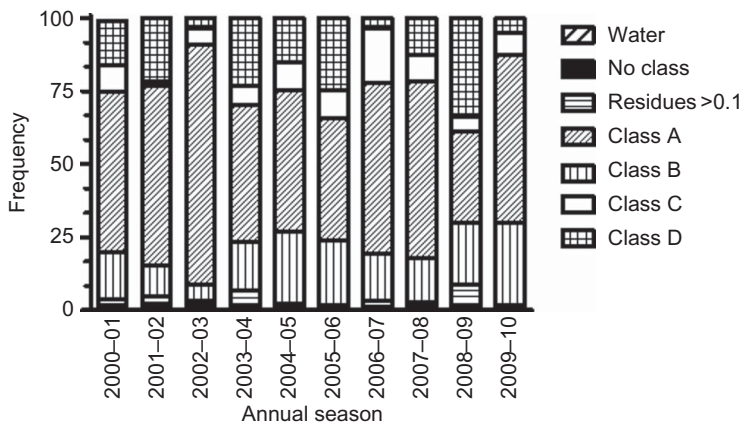


Figure 15. Frequency of the coverage of classes in the lower basin, 2000–2010.

α both current and previous mean annual rainfall (correlation coefficient = 0.75 and 0.80, respectively; $p < 0.05$). This correlation between the vegetation dynamic and rainfall conditions was observed in areas of the Humid Chaco, where shallow-rooted vegetation (Morello 1968) may have reduced capacity to access deep soil waters through the dry period (Huete et al. 2006). In the framework of this analysis, periods of drought or excessive rainfall are associated with changes in the mean value of α .

In the upper basin, Classes A and C are important in terms of spatial extent. This area is dominated by Class A, but in 2005–2006 and 2006–2007, a major decrease in Class A and increase in Class C was observed (see Figure 16). These changes are strongly correlated with positive precipitation anomalies, and were also observed for other years in the same area (2001–2002, 2004–2005, etc.). The mean differences between Classes A and C are

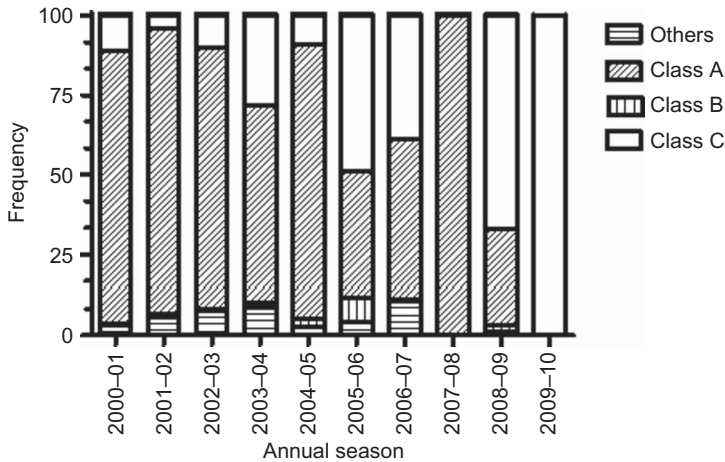


Figure 16. Frequency of the coverage of classes in the upper basin, 2000–2010.

the parameters γ (concavity of annual trend) and β (initial slope of growth). The correlation coefficient among β and γ versus mean annual rainfall ($\rho_\beta = 0.82$ and $\rho_\gamma = -0.89$, $\rho < 0.05$) was significant (correlation $\rho_\beta = 0.82$ and $\rho_\gamma = -0.89$; $p < 0.05$). Overall, the vegetation of this particular area responds to rain forcing by increased vegetation seasonality.

Finally, there were areas with higher CCI and CNI values where it was not possible to find a straightforward relationship between the observed system changes and climate drivers. This occurred in the ecotone between the Dry Chaco and Humid Chaco (boundaries of the middle and lower basins), which is usually characterized by high spatial heterogeneity and a more complex dynamics.

In summary, the analysis of NDVI patterns provided information about spatial-temporal LSP patterns. All data on pattern changes were integrated into a single map, which represents the main LSP dynamics observed in the area during the study period. The dynamics of NDVI functional forms showed three important areas (see Figure 17). The first of these was located in the middle basin, and did not show any significant changes during the 10 year period. The second site, in the upper basin, showed inter-annual variation in seasonality, with higher precipitation anomalies. The land surface phenology responded to extreme climate events giving variation in seasonality, defined as changes from Class A to C (or vice versa). In the lower basin, land surfaces differed in the magnitude of NDVI values, presenting the same seasonal trend. In this case, areas categorized as Class A changed to D (or vice versa). This result allows a better understanding of temporal change occurring in relation to climatic events (in particular, precipitation deficit).

4.2.3. Non-parabolic LSPs: agricultural frontier expansion

As discussed in Section 3.4, most areas where a good model fit was not obtained were related to biannual crops (pastures) or water. In recent years, economic and ecological factors have combined to generate a favourable environment for expansion of the agricultural frontier in the transition zone between the Yungas and the Chaco region. During the period 2002–2006, the rate of deforestation reached 1.54%, a major increase compared with the period 1998–2002 characterized by a figure of 0.69% (UMSEF 2006). Figure 18 shows the major areas affected by agricultural expansion.

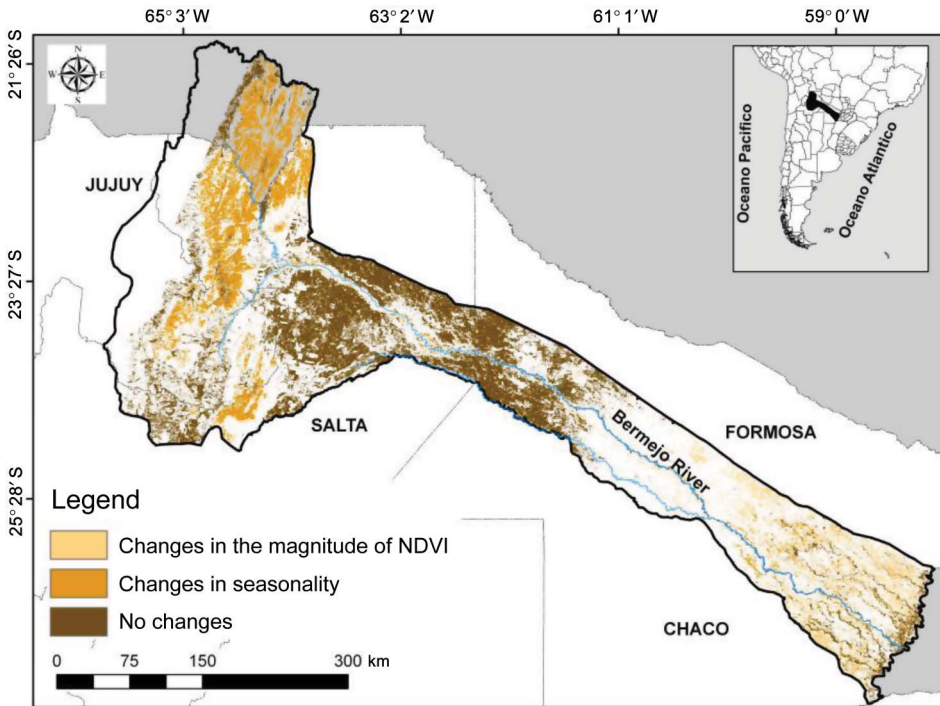


Figure 17. NDVI temporal changes related to climatic events (precipitation excess/deficit).

A good agreement was observed between UMSEF's forest inventory map and areas with high model residues. For the 2009–2010 period, agricultural expansion is evident, especially to the south.

5. Conclusions

In this work, we presented a methodology to analyse NDVI time series capable of capturing annual variation in land surface phenology in the Bermejo River basin. These results demonstrate the potential of NDVI time series analysis to monitor the temporal dynamics of vegetated surfaces, providing additional information for traditional classification and change-detection schemes. Also, the land surface phenology approach proved to be a useful framework to monitor large areas where little fieldwork is available. This methodology was specifically designed to extract information from this area, but is expected to give useful results in other areas characterized by noisy NDVI patterns. The results of classification were presented as yearly maps of the most important NDVI functional forms (annual performance of the land surface area) observed in the study area, which cover ~90% of the area.

These are the first results to derive information on rain shortage/excess effects on vegetation in northern Argentina obtained from analysis of complete MODIS NDVI time series. The seasonal NDVI pattern changes were integrated into a single map, which summarizes the inter-annual NDVI fluctuations as a function of climate forcing. In the upper basin during drought periods, NDVI values increased in the closed forest as opposed to ecosystem model predictions that water limitation should cause decline in forest canopy

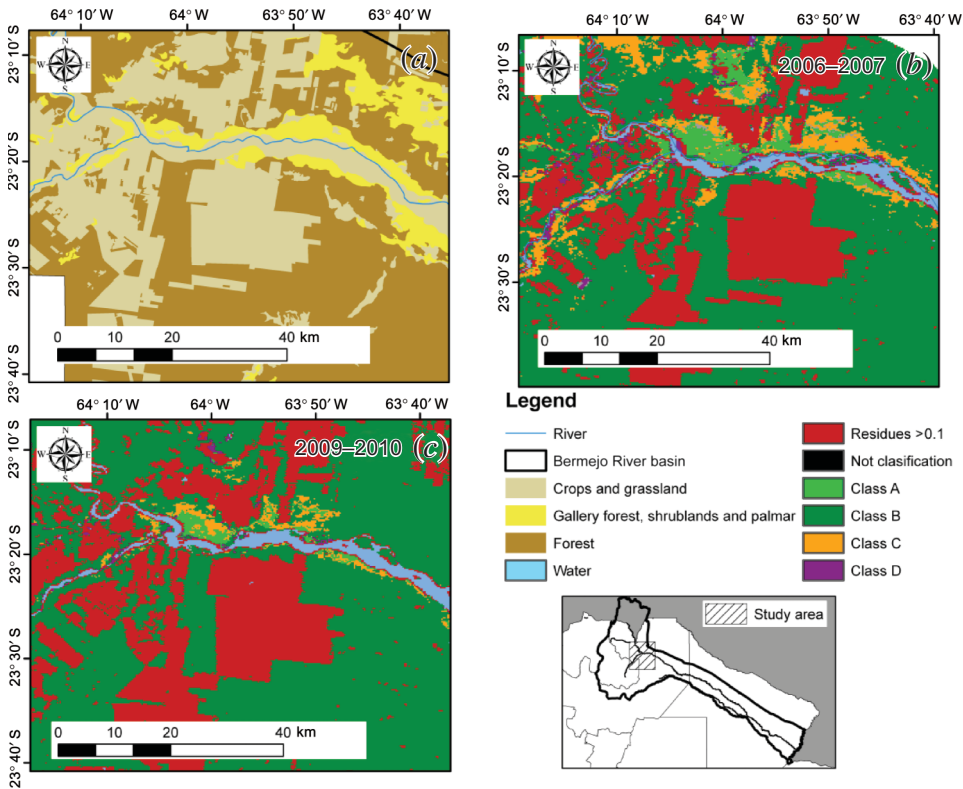


Figure 18. Comparison of crop areas. (a) Extracted from the forest inventory map (UMSEF 2006). Annual NDVI classification results for 2006–2007 (b) and 2009–2010 (c).

photosynthesis during the dry season. In contrast, areas covered with pasture and savanna (lower basin) showed dry season decline in photosynthetic capacity. The middle basin showed no fluctuation, even in periods of precipitation anomalies, because of adaptation of the characteristic vegetation to drought events. Therefore, three regions were defined: (1) areas of no change in the NDVI pattern during the study period; (2) areas with an increase in green biomass at the beginning of the growing cycle; and (3) areas with an increase in NDVI seasonality.

Nevertheless, additional work is needed in order to clarify the relations between vegetation phenology and NDVI patterns in this area. In a future work, we will include passive microwave and temperature time series data, in order to develop a more complete model of the land surface phenology in the Bermejo River basin. In particular, SAC-D/Aquarius brightness temperature data (Aquarius, L band; MWR, Ka and Ku bands) are expected to add information about foliage and branch vegetation water content. This information complements that obtained from NDVI (which is mainly related to green leaf area index (LAI)), thus reinforcing an inference strategy based on different indicators obtained by different orbital systems.

Acknowledgements

The authors wish to give special thanks to members of Unidad de Manejo del Sistema Forestal Nacional (UMSEF), Comisión Regional del Río Bermejo (COREBE) and La Administración

Provincial del Agua (APA) for their interaction and sharing of data. This work was developed within the framework of the SACD Aquarius AO 'La Plata Basin floods and droughts: Contribution of microwave remote sensing in monitoring and prediction' (MyNCIT-CONAE-CONICET project 12). The authors also wish to thank the anonymous reviewers for their valuable suggestions that significantly improved the paper.

References

- Alberto, J. A. 2005. "EcoChaco. Ambientes del Chaco." http://es.geocities.com/ja_alberto/.
- Alhamad, M. N., J. Stuth, and M. Vannucci. 2007. "Biophysical Modelling and NDVI Time Series to Project Near-Term Forage Supply: Spectral Analysis Aided by Wavelet Denoising and ARIMA Modelling." *International Journal of Remote Sensing* 28: 2513–2548.
- Anderson, M. J. 2001. "A New Method for a Non-Parametric Multivariate Analysis of Variance." *Austral Ecology* 26: 32–46.
- Baldi, G., M. D. Noretto, R. Aragón, F. Aversa, J. M. Paruelo, and E. G. Jobbágy. 2008. "Long-Term Satellite NDVI Data Sets: Evaluating their Ability to Detect Ecosystem Functional Changes in South America." *Sensors* 8: 5397–5425.
- Barros, V., E. Castañeda, and M. Doyle. 2000. "Precipitation Trends in Southern South America, East of the Andes: An Indication of Climate Variability." In *Southern Hemisphere Paleo-and Neoclimates: Key Sites, Methods, Data and Models*, edited by P. Smolka and W. Wolkheimer, 187–208. New York: Springer-Verlag.
- Barros, V., M. González, B. Liebmann, and I. Camilloni. 2000. "Influence of the South Atlantic Convergence Zone and South Atlantic Sea Surface Temperature on Inter-Annual Summer Rainfall Variability in Southeastern South America." *Theoretical and Applied Climatology* 67: 123–133.
- Box, G. E. P., and G. Jenkins. 1976. *Time Series Analysis: Forecasting and Control*. San Francisco, CA: Holden-Day.
- Brown, A. D., A. Grau, T. Lomáscolo, and N. I. Gasparri. 2002. "Una Estrategia de Conservación Para Las Selvas Subtropicales de Montaña (Yungas) de Argentina." *Ecotropicos* 15: 147–159.
- Cabido, M., C. González, A. Acosta, and S. Díaz. 1993. "Vegetation Changes Along a Precipitation Gradient in Central Argentina." *Vegetatio* 109: 5–14.
- Cabrera, Á. L. 1976. "Regiones fitogeográficas argentinas." En *Enciclopedia Argentina de Agricultura y Jardinería, Tomo 2*. 2a edición, edited by W. F. Kugler, 1–85. Buenos Aires: Acme, Fascículo 1.
- Castañeda, E. Y., and V. Barros. 1994. "Las Tendencias de La Precipitación en el Cono Sur de América al Este de Los Andes." *Meteorologica* 19: 23–32.
- Clark, M. L., T. M. Aide, H. R. Grau, and G. Riner. 2010. "A Scalable Approach to Mapping Annual Land Cover at 250 M Using MODIS Time Series Data: A Case Study in the Dry Chaco Ecoregion of South America." *Remote Sensing of Environment* 114: 2816–2832.
- De Beurs, K. M., and G. M. Henebry. 2005. "A Statistical Framework for the Analysis of Long Image Time Series." *International Journal of Remote Sensing* 26: 1551–1573.
- Fernández-Manso, A., C. Quintano, and O. Fernández-Manso. 2011. "Forecast of NDVI in Coniferous Areas Using Temporal ARIMA Analysis and Climatic Data at a Regional Scale." *International Journal of Remote Sensing* 32: 1595–1617.
- Friedl, M. A., and C. E. Brodley. 1997. "Decision Tree Classification of Land Cover from Remotely Sensed Data." *Remote Sensing of Environment* 61: 399–409.
- Giglio, L., J. Desclotres, C. O. Justice, and Y. J. Kaufman. 2003. "An Enhanced Contextual Fire Detection Algorithm for MODIS." *Remote Sensing of Environment* 87: 273–282.
- Ginzbur, G. R., and J. Adámoli. 2005. "Situación ambiental en el Chaco Húmedo." In *La Situación Ambiental Argentina*, edited by A. D. Briwn, U. Martínez Ortiz, M. Acerbi, and J. Corchera, 102–129. Buenos Aires: Argentina Fundacion Vida Silvestre.
- Ginzbur, G. R., J. Adámoli, P. Herrera, and S. Torrella. 2005. "Los Humedales del Chaco: Clasificación, Inventario y Mapeo a Escala Regional." In *Temas de la Biodiversidad del Litoral fluvial argentino II, CONICET e Instituto Miguel Lillo*, 135–152. San Miguel de Tucumán: UNT.
- González, M., E. Castañeda, and J. Teixeira Neri. 2005. "Evolución de la Precipitación en el Noreste de Argentina y Sur de Brasil." *Congremet IX*, Buenos Aires, 3–7 Octubre. ISBN 987-22411-0-4.

- González, M. H., and V. Barros. 1998. "The Relation between Tropical Convection in South America and the End of the Dry Period in Subtropical Argentina." *International Journal of Climatology* 18: 1669–1685.
- Grimm, A., V. Barros, and M. Doyle. 2000. "Climate Variability in Southern South America Associated with El Niño and La Niña Events." *International Journal of Climatology* 13: 35–58. ISSN 0894 8755.
- Hird, J. N., and G. J. Mcdermid. 2009. "Noise Reduction of NDVI Time Series: An Empirical Comparison of Selected Techniques." *Remote Sensing of Environment* 113: 248–258.
- Huete, A. R., K. Didan, T. Miura, E. Rodriguez, X. Gao, and L. Ferreira. 2002. "Overview of the Radiometric and Biophysical Performance of the MODIS Vegetation Indices." *Remote Sensing of Environment* 83: 195–213.
- Huete, A. R., K. Didan, Y. E. Shimabukuro, P. Ratana, S. R. Saleska, L. R. Hutya, W. Yang, R. R. Nemani, and R. Myneni. 2006. "Amazon Rainforests Green-up with Sunlight in Dry Season." *Geophysical Research Letters* 33: L06405.
- Huete, A., C. Justice, and W. V. Leeuwen. 1999. *EOS MODIS Vegetation Index (MOD 13) Theoretical Basis Document*. p. 115. Greenbelt, MD: University of Virginia, NASA Goddard Space Flight Center.
- Jönsson, P., and L. Eklundh. 2004. "TIMESAT—A Program for Analyzing Time-Series of Satellite Sensor Data." *Computers and Geoscience* 30: 833–845.
- Julien, Y., and J. A. Sobrino. 2009. "Global Land Surface Phenology Trends from GIMMS Database." *International Journal of Remote Sensing* 30: 3495–3513.
- Kiladis, G., and H. Diaz. 1989. "Global Climatic Anomalies Associated with Extremes in the Southern Oscillation." *International Journal of Climatology* 2: 1069–1090. ISSN 0894 8755.
- Leeuwen Van, W. J. D., A. R. Huete, K. Didan, and T. Laing. 1997. "Modeling Bidirectional Reflectance Factors for Different Land Cover Types and Surface Components to Standardize Vegetation Indices." In *Proceedings of the 7th International Symposium on Physical Measurements and Signatures in Remote Sensing*, Courcheval, April 7–11, 1997, 373–380.
- Liang, L., and M. Schwartz. 2009. "Landscape Phenology: An Integrative Approach to Seasonal Vegetation Dynamics." *Landscape Ecology* 24: 465–472.
- Minetti, J. L. 1999. *Atlas Climático del Noroeste Argentino* Laboratorio Climatológico Sudamericano, Fundación Zon Caldenius, Tucumán, Argentina.
- Moody, E. G., M. D. King, S. Platnick, C. B. Schaff, and F. Gao. 2005. "Spatially Complete Global Spectral Surface Albedos: Value-Added Datasets Derived from Terra MODIS Land Products." *IEEE Transaction on Geoscience and Remote Sensing* 43: 144–158.
- Morello, J. 1968. *La vegetación de la República Argentina*, No. 10: Las Grandes Unidades de Vegetación y Ambiente del Chaco Argentino, Buenos Aires, Argentina.
- Morello, J., and J. Adámoli. 1974. "Las Grandes Unidades De Vegetación Y Ambiente Del Chaco Argentino II. Vegetación Y Ambiente De La Provincia Del Chaco. INTA." *Serie Fitogeográfica* 13: 1–130.
- Myneni, R. B., C. Keeling, C. Tucker, G. Asrar, and R. Nemani. 1997. "Increased Plant Growth in the Northern High Latitudes from 1981 to 1991." *Nature* 386: 698–702.
- Pettorelli, N., J. O. Vik, A. Mysterud, J.-M. Gaillard, C. J. Tucker, and N. C. Stenseth. 2005. "Using the Satellite-Derived NDVI to Assess Ecological Responses to Environmental Change." *Trends in Ecology & Evolution* 20: 503–510.
- Reboita, M. S., M. A. Gan, R. P. Da Rocha, and T. Ambrizzi. 2010. "Regimes De Precipitacao Na America Do Sul." *Revista Brasileira De Meteorologia* 25: 185–204. ISSN 0102–7786.
- Reed, B. C., J. F. Brown, D. Vanderzee, T. R. Loveland, J. W. Merchant, and D. O. Ohlen. 1994. "Measuring Phenological Variability from Satellite Imagery." *Journal of Vegetation Science* 5: 703–714.
- Revadekar, J. V., Y. K. Tiwari, and K. R. Kumar. 2012. "Impact of Climate Variability on NDVI Over the Indian Region During 1981–2010." *International Journal of Remote Sensing* 33: 7132–7150.
- Ropelewski, C., and M. Halpert. 1987. "Global and Regional Scale Precipitation Patterns Associated with El Niño." *Monthly Weather Review* 110: 1606–1626. ISSN 0027–0644.
- Sobrino, J. A., and Y. Julien. 2011. "Global Trends in NDVI-Derived Parameters Obtained from GIMMS Data." *International Journal of Remote Sensing* 32: 4267–4279.
- Tan, B., J. T. Morissette, R. E. Wolfe, F. Gao, G. A. Ederer, J. Nightingale, and J. A. Pedelty. 2011. "An Enhanced TIMESAT Algorithm for Estimating Vegetation Phenology Metrics from MODIS Data." *IEEE Journal of Selected Topics in Applied Earth Observations and Remote Sensing* 4: 361–371.

- Torella, S. A., and J. Adamoli. 2005. "Situacion Ambiental De La Ecoregion Del Chaco Seco." In *Situacion Ambiental Argentina*, edited by A. D. Briwn, U. Martinez Ortiz, M. Acerbi, and J. Corchera, 75–82. Buenos Aires: Argentina Fundacion Vida Silvestre.
- Tucker, C. J., D. A. Slayback, J. E. Pinzon, S. O. Los, R. B. Myneni, and M. G. Taylor. 2001. "Higher Northern Latitude Normalized Difference Vegetation Index and Growing Season Trends From 1982 to 1999." *International Journal of Biometeorology* 45: 184–190.
- UMSEF. 2006. *Monitoreo De Bosque Nativo Periodo 1998–2002/Periodo 2002–2006 (Datos Preliminares)*. Dirección De Bosques Secretaría De Ambiente Y Desarrollo Sustentables. Buenos Aires: Dirección de Bosques, SAyDS, Ministerio de Salud y Ambiente.
- Verbesselt, J., R. Hyndman, A. Zeileis, and D. Culvenor. 2010. "Phenological Change Detection While Accounting for Abrupt and Gradual Trends in Satellite Image Time Series." *Remote Sensing of Environment* 114: 2970–2980.
- Vermote, E. F., N. Z. El Saleous, and C. O. Justice. 2002. "Atmospheric Correction of MODIS Data in the Visible to Middle Infrared: First Results." *Remote Sensing of Environment* 83: 97–111.
- Vermote, E. F., N. Z. El Saleous, C. O. Justice, Y. J. Kaufman, J. L. Privette, and L. Remer. 1997. "Atmospheric Correction of Visible to Middle-Infrared EOS-MODIS Data Over Land Surfaces: Background, Operational Algorithm and Validation." *Journal of Geophysical Research* 102: 17131–17141.
- Vermote, E. F., and A. Vermeulen. 1999. "Atmospheric Correction Algorithm: Spectral Reflectances (MOD09)." Algorithm Theoretical Background Document. http://modarch.gsfc.nasa.gov/MODIS/ATBD/atbd_mod08
- Walthall, C. L. 1997. "A Study of Reflectance Anisotropy and Canopy Structure Using a Simple Empirical Model." *Remote Sensing of Environment* 61: 118–128.
- Wolfe, R. E., D. P. Roy, and E. F. Vermote. 1998. "MODIS Land Data Storage, Gridding, and Compositing Methodology: Level 2 Grid." *IEEE Transaction on Geoscience and Remote Sensing* 36: 1324–1338.
- Xiao, X., B. Braswell, Q. Zhang, S. Boles, S. Frolking, and B. Moore. 2003. "Sensitivity of Vegetation Indices to Atmospheric Aerosols: Continental-Scale Observations in Northern Asia." *Remote Sensing of Environment* 84: 385–392.
- Zak, M. R., M. Cabido, D. Cáceres, and S. Díaz. 2008. "What Drives Accelerated Land Cover Change in Central Argentina? Synergistic Consequences of Climatic, Socioeconomic, and Technological Factors." *Environmental Management* 42: 181–189.
- Zhang, X., M. A. Friedl, C. B. Schaaf, A. H. Strahler, J. C. F. Hodges, F. Gao, B. C. Reed, and A. Huete. 2003. "Monitoring Vegetation Phenology Using MODIS." *Remote Sensing of Environment* 84: 471–475.
- Zhou, L., R. Kaufmann, Y. Tian, R. Myneni, and C. Tucker. 2003. "Relation between Inter-Annual Variations in Satellite Measures of Northern Forest Greenness and Climate between 1982 and 1999." *Journal of Geophysical Research* 108 (D1): 4004.